NASA MEMO 2-4-59L

NASA

MEMORANDUM

EXPERIMENTAL INFLUENCE COEFFICIENTS AND VIBRATION MODES OF A MULTISPAR 60° DELTA WING

By Deene J. Weidman and Eldon E. Kordes

Langley Research Center
Langley Field, Va.

NATIONAL AERONAUTICS AND SPACE ADMINISTRATION
WASHINGTON
May 1959

NATIONAL AERONAUTICS AND SPACE ADMINISTRATION

MEMORANDUM 2-4-59L

EXPERIMENTAL INFLUENCE COEFFICIENTS AND VIBRATION MODES OF A MULTISPAR 60° DELTA WING

By Deene J. Weidman and Eldon E. Kordes

SUMMARY

Test results are presented for both symmetrical and antisymmetrical static loading of a wing model mounted on a three-point support system. The first six free-free vibration modes were determined experimentally. A comparison is made of the symmetrical nodal patterns and frequencies with the symmetrical nodal patterns and frequencies calculated from the experimental influence coefficients.

INTRODUCTION

The design analysis of low-aspect-ratio wings is particularly troublesome because of the difficulties involved in determining their stiffness characteristics. Recently several methods of analysis of wing structures have been proposed. (See, for example, refs. 1 to 4.) However, few data are available for assessing these theories. Static- and vibration-test results are available for a 45° built-up delta-wing specimen with ribs normal to the spars (ref. 5). In order to provide experimental information on the deflectional characteristics of delta wings with another type of internal construction, static and vibration tests were conducted on a 60° delta wing with skewed ribs and spars. The experimental results of these tests are presented in the form of static influence coefficients and vibration modes and frequencies. The static influence coefficients were measured for both symmetrical and antisymmetrical loading with the wing on a three-point support. The first six frequencies and corresponding nodal patterns were measured for the wing in an essentially free-free condition. In addition, the first three symmetrical mode shapes and frequencies were calculated from the experimental influence coefficients.

DESCRIPTION OF SPECIMEN

The specimen used in these tests is the 60° delta wing shown in figures 1 and 2. The wing has a waffle-like skin made of 7075-T6 aluminum alloy riveted to a rib-spar framework made of 2024-T3 aluminum alloy. The span of the wing is 96.5 inches and the root chord is 89.25 inches. The maximum overall depth varies linearly from 4.52 inches at the center line to 1.22 inches at the tip. A typical chordwise section is shown in figure 2(a). The internal construction as shown in figure 2(b) consists of eleven streamwise ribs and five spars. Four spars were skewed and one spar at the trailing edge was normal to the ribs. The spar and rib components are identified with part numbers to facilitate reference, spars being referred to as parts 1 to 5 and rib components as parts 6 to 26. Spar 1 is continuous across the wing center line. Rib 6 is a 4-inch aluminum-alloy I-beam with a 2-inch flange and a uniform thickness of 1/8 inch. Detailed dimensions of the internal construction are given in table 1. In this table all dimensions except thicknesses are given as nominal values. The internal construction and cover before assembly are shown in figure 3.

In order to facilitate any future analyses the area moments of inertia of both the spars and ribs were calculated. The values of the moments of inertia at the points of intersection of the spars and ribs are given in table 2. The part numbers shown are identified in figure 2(b).

The waffle covers were made by machining square indentations in a tapered plate. The dimensions of the covers are shown in figure 2(c). The overall cover depth varies linearly in the spanwise direction from 0.489 inch at the root to 0.122 inch at the tip. Since the skin thickness depended entirely on the depth of the square indentation, extreme difficulty in controlling this depth resulted in large variations in skin thickness. This is illustrated in figure 4, where the spanwise variations of skin thicknesses are shown for each of the four semispan cover sheets. Each thickness shown is the average of the measured thicknesses along the corresponding chord. It should be mentioned that the random variation of skin thicknesses along the chord is similar to the spanwise variation. These spanwise thickness variations were replaced by a straight line through the use of a least square method which gave a skin thickness variation of from 0.042 inch at the root to 0.030 inch at the tip.

STATIC TESTS

Static tests were conducted on the wing specimen in order to obtain symmetrical and antisymmetrical influence coefficients. For these tests the wing specimen was mounted on three supports which restrained normal displacement of the wing at the supports but allowed rotation. The advantages of this type of support are that the same support fixtures may be used for both the symmetrical and antisymmetrical loading conditions, and also the influence coefficients appropriate to other support conditions can be calculated from the influence coefficients obtained for the three-point support.

Test Setup

A general view of the static test setup is shown in figure 5. The two rear supports were located along the trailing edge at the intersections of the first and second spars and the forward support was located at the intersection of the forward spar and center rib. These support fixtures are illustrated in figure 6. The forward support consisted of a roller attached to a support fixture above the wing and a steel plate attached to the wing. The wing was held firmly against the roller by a weight-lever counterbalancing system. The rear supports consisted essentially of a pin connection between a bracket attached to the rear spar and a pedestal bolted to the floor. Self-alining bearings were used to permit spanwise as well as chordwise rotation.

Loads were applied to the wing by means of hydraulic jacks which were fitted with screw locks so that, once a given applied load was reached hydraulically, it could be maintained mechanically. Standard strain-gage load cells placed between the wing and the jacks were used to determine the applied loads. For the antisymmetrical tests, an overhead loading support fixture was constructed to allow loads to be applied to the top surface of the wing. This fixture can be seen in the foreground of figure 5.

The deflections of the wing were measured by means of dial gages. Gages were also mounted at the supports to afford a measurement of the support movement. The dial gages used had a minimum reading of 0.0001 inch with a 0.5-inch maximum travel. Accuracy of these gages was better than ±0.0005 inch.

Test Procedure and Results

Deflections were measured at the stations shown in figure 7 under both symmetrical and antisymmetrical loading conditions. For both conditions loads were applied to each of the stations in succession, and for each loading gage readings were taken at an initial preload and at each of three equal load increments. Maximum loads were chosen so that no buckling or local crippling occurred and also so that the maximum deflection did not exceed the range of the dial gages (0.5 inch). The condition of no local failure limited the loads that could be applied along the leading edge (forward of spar 5) to such low values that accurate deflection data could not be obtained for these loads.

As might be expected, the supports deflected under loading so that a rigid-body correction for these deflections was necessary. Inasmuch as the rear supports were placed far outboard of the center line and the forward support was near the tip, these corrections were based on support deflections alone and consisted of a superposition of three types of rigid-body motion; namely, roll, pitch, and translation.

Since the deflections at the various stations appeared to be a nearly linear function of the load, a straight line was drawn for the load-deflection curve by means of a least-squares criterion. The slope of this straight line was used to extrapolate the load-deflection curve to a 1,000-pound load. For the case of symmetrical loading on the three-point support system, the resulting deflections in the form of an influence-coefficient matrix are shown in table 3. In order that the matrix be a symmetrical matrix, each value given in table 3 is the average of the two cross-coupling coefficients. Deviations from the mean are given in parenthesis, the largest deviation being 0.013 inch or 3.0 percent of the maximum deflection.

The influence coefficients for the antisymmetrical loading case were similarly determined and are shown in table 4, where each value given is for a 1,000-pound load. Each value is the average of the two cross-coupling terms, with the deviations from the mean shown in parenthesis. The largest deviation in these influence coefficients is 0.028 inch or 5.3 percent of the maximum deflection. Loads were not applied at station 24 because of the inability of the wing to sustain sufficient loads at that station to allow a reasonably accurate extrapolation to 1,000 pounds. Values shown for this station are the deflections at station 24 due to 1,000-pound loads elsewhere. The deflection of station 24 due to a 1,000-pound load at station 24 was not measured.

VIBRATION TESTS

Test Equipment

The model was vibrated by means of a shaker system. This shaker system consists of a set of electromagnetic shakers, a control console, and a rotating-machine power supply with a frequency range of 5 to 500 cycles per second. Each shaker has a controlled force amplitude from 0 to 50 pounds and a phase control (0° or 180°) over the available frequency range. The total weight of the moving element of each shaker, including a velocity-sensitive signal generator or pickup, is 2.0 pounds. A more complete description of this equipment is given in references 5 and 6. The equipment used for the present tests consisted of response-measuring instruments and two electromagnetic shakers.

The motion of the specimen at resonance was obtained with a portable probe pickup, whose output was viewed on a cathode-ray oscilloscope. The frequency of vibration was obtained from a Stroboconn frequency indicator.

Test Setup

An overall view of the vibration test setup is shown in figure 8. The wing was suspended from a wooden frame by a flexible steel cable attached to the forward tip of the root chord. This method of support allows essentially free-free vibration in the horizontal direction. The shakers were placed on the floor and attached to the trailing-edge spar at a point 6 inches inboard of the junction with the second spar. In order to tune out troublesome resonances of the support cable, a small movable mass was attached to the cable.

Test Procedure and Results

For these tests the phase controls were set to produce the desired motion of the wing (symmetrical or antisymmetrical about the center line). The power supply was turned on and the force outputs of the shakers were equalized. The force output being held constant, the frequency was slowly increased until the amplitude of vibration reached a maximum. In order to observe the motion of the wing, the output of one signal generator was put on the horizontal axis of the oscilloscope and the shaker force signal (current through the shaker drive coil) was switched onto the vertical axis. The resulting Lissajous ellipse shown on the oscilloscope was used as an aid in determining the resonant frequency. The frequency was then read off the frequency indicator and recorded. With the wing still held at resonance, the probe pickup was connected to the oscilloscope and an amplitude survey of the wing was made in order to locate the associated node lines. After the nodal pattern and frequency were established and the data recorded, the frequency was increased until the next resonance was detected. In this manner the first 6 natural modes of the specimen were identified and recorded. Higher modes were not readily discernible because of panel vibrations in the skin and, hence, only the lower modes were determined. The natural frequencies and associated nodal patterns are shown in figure 9(a) for the symmetrical modes, and in figure 9(b) for the antisymmetrical modes.

CALCULATED MODES

The mode shapes and frequencies of the 60° delta wing specimen vibrating symmetrically in a free-free condition were calculated from the influence coefficients for the three-point support condition by the manner outlined in reference 7.

For these calculations the distribution of mass to the various stations shown in figure 7 had to be made. The masses (in pound units) of all the component parts of the wing were calculated on the basis of the dimensions of the wing given in figure 2 and table 1 with the exception of the skin thickness, where actual measured thicknesses were used. The distribution was then calculated in the following manner (see sketch):

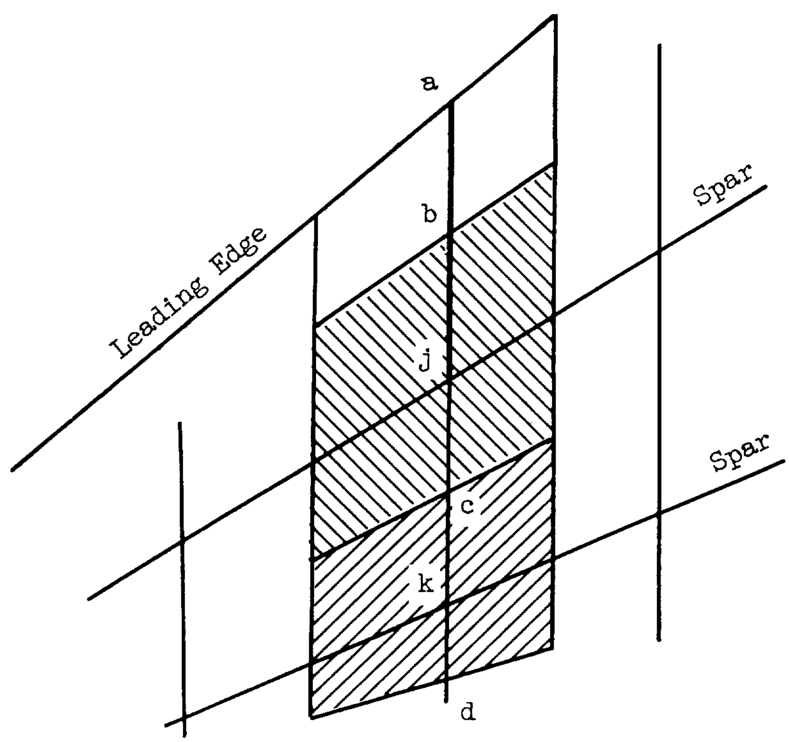

For a typical inboard station j, all the material located within the trapezoidal shaded area containing j was considered uniformly distributed along the line bc. For leading-edge stations the material located within the trapezoidal area near the leading edge was considered uniformly distributed along the line ab. These sectionally uniform distributions were then allocated to the particular chordwise stations as shown in the sketch below:

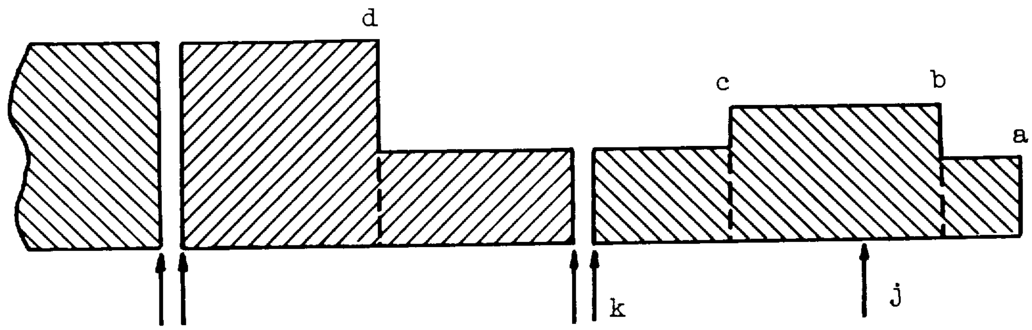

Each rib element was treated as a simple beam between stations with the sectionally uniform weight distribution considered as a loading. The reactions calculated at each station were then considered to be the mass associated with the station. This process was used in order to take into account at least some effect of the overhanging leading edge at the outboard ribs. The masses associated with each station are tabulated in table 5.

From this mass distribution and the experimental influence coefficients, the first three symmetrical modes and frequencies were calculated, and the results are shown in figure 10. A comparison of the measured frequencies and their associated node lines with the same quantities determined from calculations based on the influence coefficients can be made by comparing figures 9(a) and 10. The experimental and calculated frequencies are seen to agree within 10 percent for the lowest three symmetrical modes. The calculated nodal patterns of the first two modes have the same general shape as the first two experimental nodal patterns. However, the calculated nodal pattern of the third mode is quite different from the experimental nodal pattern. This difference is believed to be due primarily to the absence of experimental influence coefficients for the region along the leading edge. Since the leading-edge region of the wing represents a large portion of this structure, the lack of influence coefficients in this region would be expected to have an appreciable effect on the nodal patterns, especially in the higher modes. Also, some of the differences between the calculated and experimental nodal patterns and frequencies might be due to extreme variations in waffle skin dimensions which directly affect the mass distribution and to the large overhanging leading edge which necessitated an approximate mass distribution as indicated above. Since the difficulties involved in calculating the antisymmetrical modes and frequencies are of the same character as those encountered in the symmetrical case and since the antisymmetrical results probably would not present any additional information, the antisymmetrical modes and frequencies were not calculated.

CONCLUDING REMARKS

The stiffness characteristics of a 60° delta wing were obtained in the form of influence coefficients and natural modes and frequencies. Comparisons show that the measured frequencies and those calculated using the measured influence coefficients agreed within 10 percent for the three lowest symmetrical modes.

Langley Research Center,
National Aeronautics and Space Administration,
Langley Field, Va., October 24, 1958.

REFERENCES

1. Stein, Manuel, and Sanders, J. Lyell, Jr.: A Method for Deflection Analysis of Thin Low-Aspect-Ratio Wings. NACA TN 3640, 1956.

2. Schuerch, H. U., and Freelin, J. R.: Structural Analysis of a Delta Wing Structure by Elastic Coefficients. Rep. No. ZS-182, Convair, May 5, 1953.

3. Levy, Samuel: Structural Analysis and Influence Coefficients for Delta Wings. Jour. Aero. Sci., vol. 20, no. 7, July 1953, pp. 449-454.

4. Williams, D.: Recent Developments in the Structural Approach to Aeroelastic Problems. Jour. R.A.S., vol. 58, June 1954, pp. 403-428.

5. Kordes, Eldon E., Kruszewski, Edwin T., and Weidman, Deene J.: Experimental Influence Coefficients and Vibration Modes of a Built-Up 45° Delta-Wing Specimen. NACA TN 3999, 1957.

6. Kordes, Eldon E., and Kruszewski, Edwin T.: Experimental Investigation of the Vibrations of a Built-Up Rectangular Box Beam. NACA TN 3618, 1956.

7. Kruszewski, Edwin T., and Waner, Paul G., Jr: Evaluation of the Levy Method as Applied to Vibrations of a 45° Delta Wing. NASA MEMO 2-2-59L, 1959.

TABLE 1.- DIMENSIONS OF INTERNAL COMPONENTS FOR SEMISPAN OF MODEL

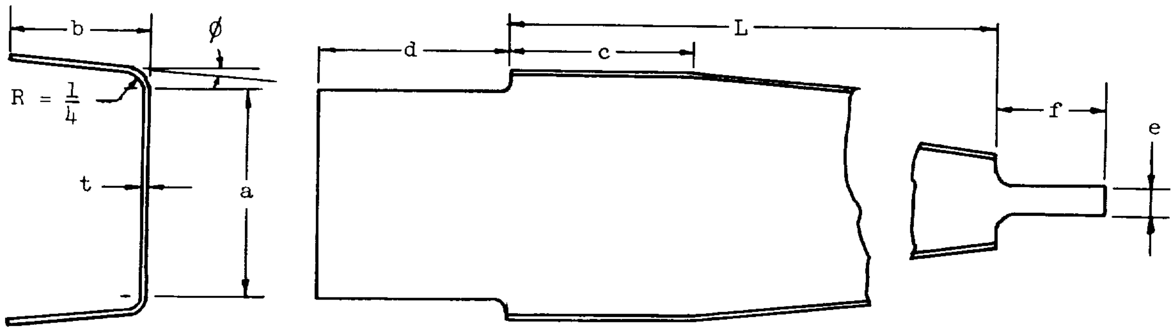

Part (See fig. 2(b))	L, in.	a, in.	b, in.	c, in.	d, in.	e, in.	f, in.	∅, deg	t, in.
Spars									
[a]1	48.250	1.09	0.750	44.406	0	0.48	0	4.5	0.0795
2	38.250	3.62	.750	0	3.541	1.21	3.000	5	.0810
3	54.875	2.79	1.125	0	3.621	.38	1.622	0	.0650
4	64.800	2.77	.750	0	4.196	.36	1.696	0	.0638
5	76.425	3.65	.750	0	5.164	.48	0	1.5	.0808
Rib Components									
[b]6	88.250	----	-----	------	-----	----	-----	---	------
7	12.125	2.43	0.750	0	1.791	0.35	1.893	0	0.0803
7a	13.000	2.47	.750	0	2.291	.31	1.893	0	.0799
8	13.375	2.43	.750	0	1.870	2.43	2.665	2	.0803
8a	13.625	2.52	.750	0	1.791	2.52	2.747	2	.0810
9	15.250	2.46	.750	0	2.540	2.46	2.696	2	.0643
10	16.250	2.46	.750	0	1.696	2.46	2.664	2	.0647
11	11.250	2.46	.750	0	1.664	.66	0	6	.0645
12	8.250	1.89	.750	0	2.041	.53	1.893	0	.0642
13	10.875	1.98	.750	0	1.791	1.98	2.871	2	.0630
14	13.250	1.98	.750	0	1.746	1.98	2.446	2	.0629
15	13.500	2.01	.750	0	1.696	2.01	2.414	2	.0515
16	10.625	2.01	.750	0	1.664	.30	0	6	.0516
17	3.750	1.37	.750	0	2.041	.73	1.893	0	.0510
18	8.437	1.45	.750	0	1.791	1.45	2.871	2	.0521
19	9.625	1.45	.750	0	1.746	1.45	2.446	2	.0521
20	10.375	1.47	.750	0	1.696	1.47	2.414	2	.0407
21	6.375	1.47	.750	0	1.664	.45	0	6	.0409
22	6.500	.91	.750	0	2.246	.91	1.893	2	.0519
23	6.375	.91	.750	0	1.746	.91	2.196	2	.0409
24	7.750	.91	.750	0	1.696	.91	2.164	2	.0409
25	3.500	.91	.750	0	1.664	.48	0	6	.0407
26	9.676	.35	.750	0	2.686	.35	1.893	2	.0513

[a]Spar 1 is continuous over the full span.
[b]Four-inch I-beam (see fig. 2(b)).

TABLE 2.- AREA MOMENTS OF INERTIA, I, OF THE SPARS AND RIBS ABOUT THEIR CENTROIDS

Spars			Ribs		
Part (see fig. 2(b))	Location, percent semispan	I, in.^{4}	Part (see fig. 2(b))	Location, percent semispan	I, in.^{4}
1	0.000	0.11673	6	0.000	0.16015
	1.000	.04149		.500	1.82487
2	.000	1.02374		1.000	.20247
	.171	.79207	7	.000	.02048
	.427	.51220		1.000	.32138
	.727	.27493	7a	.000	.01855
	1.000	.13184		1.000	.33074
3	.000	.60881	8	.500	.31860
	.130	.48454	8a	.500	.34642
	.327	.32791	9	.500	.26281
	.558	.18867	10	.500	.27043
	.789	.09206	12	.000	.02379
	1.000	.03631		1.000	.15703
4	.000	.44639	13	.500	.16667
	.124	.35518	14	.500	.16641
	.321	.23601	15	.500	.14082
	.550	.13320	17	.000	.02734
	.779	.06368		1.000	.06998
	1.000	.02313	18	.500	.07768
5	.000	.99542	19	.500	.07768
	.127	.77492	20	.500	.06220
	.314	.51126	22	.500	.03678
	.540	.27881	23	.500	.02890
	.767	.12619	24	.500	.02890
	1.000	.03839	26	.500	.01395

TABLE 3.- INFLUENCE COEFFICIENTS FOR THE WING ON A THREE-POINT

[Stations are identified

Deflection station	Load (a)												
	1	2	3	4	6	7	8	9	10	11	12	13	14
1	0.434	(0.001) .299	(-0.005) .203	(-0.004) .092	(-0.008) -.074	(0.002) .385	(0.003) .290	(0.001) .206	(-0.009) .117	(0.001) .037	(0.004) .302	(0.008) .254	(-0.001) .208
2	(-.002) .299	.257	(-.005) .194	(-.002) .094	(-.005) -.076	(.004) .279	(.003) .237	(.002) .187	(-.005) .122	(.001) .040	(.003) .223	(.008) .202	(-.001) .182
3	(.004) .203	(.005) .194	.180	(.001) .095	(.006) -.065	(.006) .189	(.006) .178	(.003) .160	(-.001) .115	(.001) .040	(.003) .152	(.010) .149	(.003) .150
4	(.003) .092	(.002) .094	(-.002) .095	.068	(-.010) -.060	(.004) .086	(.004) .085	(.002) .083	(.002) .074	(.008) .035	(.005) .071	(.005) .072	(.001) .078
6	(.008) -.074	(.005) -.076	(-.005) -.065	(.009) -.060	.144	(.006) -.069	(.007) -.074	(.006) -.071	(.007) -.063	(.001) -.022	(.006) -.058	(.004) -.060	(.007) -.068
7	(-.002) .385	(-.005) .279	(-.007) .189	(-.004) .086	(-.006) -.069	.363	(.001) .274	(-.001) .193	(-.007) .115	(.000) .035	(-.008) .307	(.004) .245	(-.003) .197
8	(-.003) .290	(-.002) .237	(-.005) .178	(-.003) .085	(-.006) -.074	(-.002) .274	.236	(.000) .182	(-.006) .114	(-.001) .036	(.000) .224	(.005) .206	(-.003) .180
9	(-.002) .206	(-.001) .187	(-.004) .160	(-.001) .083	(-.007) -.071	(.001) .193	(.000) .182	.171	(-.004) .115	(-.001) .040	(.001) .160	(.003) .157	(-.002) .164
10	(.009) .117	(.005) .122	(.001) .115	(-.002) .074	(-.006) -.063	(.007) .115	(.005) .114	(.004) .115	.108	(.001) .043	(.006) .096	(.007) .099	(.003) .112
11	(-.001) .037	(-.001) .040	(-.001) .040	(-.009) .035	(-.001) -.022	(.000) .035	(.002) .036	(.001) .040	(-.001) .043	.035	(.001) .029	(.002) .032	(.003) .041
12	(-.004) .302	(-.002) .223	(-.003) .152	(-.004) .071	(-.006) -.058	(.008) .307	(.000) .224	(-.001) .160	(-.006) .096	(.000) .029	.278	(.004) .211	(-.004) .166
13	(-.009) .254	(-.008) .202	(-.009) .149	(-.004) .072	(-.004) -.060	(-.005) .245	(-.005) .206	(-.004) .157	(-.007) .099	(-.001) .032	(-.005) .211	.200	(-.006) .167
14	(.001) .208	(.001) .182	(-.003) .150	(-.002) .078	(-.006) -.068	(.003) .197	(.004) .180	(.002) .164	(-.004) .112	(-.003) .041	(.004) .166	(.006) .167	.185
15	(.002) .149	(.001) .142	(-.002) .127	(-.001) .073	(-.004) -.066	(.003) .142	(.005) .138	(.002) .134	(-.003) .115	(.000) .047	(.004) .118	(.006) .123	(.000) .145
16	(.002) .089	(.001) .091	(-.002) .086	(.000) .052	(-.002) -.049	(.003) .084	(.004) .086	(.003) .087	(.000) .082	(-.001) .050	(.004) .070	(.005) .077	(.004) .090
17	(-.002) .160	(-.002) .120	(-.003) .083	(-.001) .038	(-.002) -.032	(.001) .159	(-.001) .120	(.001) .086	(-.002) .052	(.000) .016	(.000) .156	(.003) .120	(.000) .092
18	(.004) .183	(-.003) .136	(-.002) .103	(-.001) .050	(-.005) -.041	(.004) .175	(.003) .145	(.001) .110	(-.002) .069	(.001) .022	(.005) .159	(.007) .145	(.003) .125
19	(.002) .165	(.000) .143	(-.003) .116	(-.002) .059	(-.007) -.052	(.003) .159	(.004) .142	(.001) .127	(-.004) .086	(-.002) .032	(.004) .138	(.000) .133	(-.003) .150
20	(.005) .155	(.003) .143	(-.001) .124	(-.001) .069	(-.011) -.055	(.006) .147	(-.007) .128	(.003) .132	(-.002) .103	(.000) .041	(.007) .125	(.009) .129	(.002) .148
21	(.002) .125	(.001) .124	(.000) .112	(.000) .066	(-.002) -.060	(.004) .118	(.006) .118	(.003) .118	(-.001) .102	(.000) .049	(.006) .100	(.008) .108	(.004) .127
23	(-.004) .054	(.002) .057	(.000) .050	(.000) .027	(-.011) -.030	(.005) .060	(.004) .057	(.002) .053	(-.001) .040	(.012) .025	(.005) .051	(.007) .057	(.002) .063
24	(.001) .101	(.000) .097	(-.002) .085	(-.001) .048	(-.005) -.041	(.002) .096)	(.003) .095	(.000) .090	(-.005) .070	(-.001) .025	(.003) .081	(.005) .088	(-.002) .101
25	(.001) .109	(.000) .109	(-.002) .099	(-.001) .058	(-.005) -.050	(.002) .103	(.003) .104	(.000) .105	(-.004) .086	(-.002) .035	(.004) .087	(.005) .097	(.001) .115
26	(.007) -.055	(.006) -.035	(.003) -.018	(.002) -.007	(-.003) .009	(.008) -.054	(.010) -.033	(.004) -.020	(.001) -.008	(.001) -.003	(.007) -.052	(.008) -.036	(.002) -.024
27	(.007) -.055	(.006) -.035	(.003) -.018	(.002) -.007	(-.003) .009	(.008) -.054	(.010) -.033	(.004) -.020	(.001) -.008	(.001) -.003	(.007) -.052	(.008) -.036	(.002) -.024
28	(.007) -.009	(.006) .006	(.002) .016	(.003) .015	(-.005) -.008	(.007) -.011	(.005) .004	(.002) .016	(-.001) .017	(.000) .005	(.006) -.015	(.007) .002	(.003) .019
29	(.006) .028	(.004) .040	(.000) .045	(.000) .028	(-.011) -.015	(.006) .025	(.006) .038	(.001) .047	(-.003) .041	(-.001) .015	(.005) .019	(.007) .035	(-.006) .060

[a]Values in parentheses are deviations from the mean value.

SUPPORT SYSTEM BASED ON A 1,000-POUND SYMMETRICAL LOAD

in figure 7]

station													
15	16	17	18	19	20	21	23	24	25	26	27	28	29
(-0.002) .149	(-0.001) .089	(0.003) .160	(-0.005) .183	(-0.002) .165	(-0.005) .155	(-0.003) .125	(0.003) .054	(-0.001) .101	(-0.002) .109	(-0.007) -.055	(-0.007) -.055	(-0.007) -.009	(-0.006) .028
(.000) .142	(-.001) .091	(.001) .120	(.004) .136	(.000) .143	(-.003) .143	(-.002) .124	(-.002) .057	(.000) .097	(.000) .109	(-.006) -.035	(-.006) -.035	(-.005) .006	(-.003) .040
(.002) .127	(.003) .086	(.002) .083	(.002) .103	(.002) .116	(.000) .124	(.001) .112	(-.001) .050	(.002) .085	(.002) .099	(-.004) -.018	(-.004) -.018	(-.003) .016	(.000) .045
(.001) .073	(-.001) .052	(.001) .038	(.001) .050	(.002) .059	(.002) .069	(.000) .066	(.000) .027	(.001) .048	(.000) .058	(-.001) -.007	(-.001) -.007	(-.004) .015	(.000) .028
(.005) -.066	(.002) -.049	(.003) -.032	(.005) -.041	(.008) -.052	(.010) -.055	(.003) -.060	(.011) -.030	(.005) -.041	(.004) -.050	(.003) .009	(.003) .009	(.005) -.008	(.010) -.015
(-.004) .142	(-.003) .084	(.000) .159	(-.004) .175	(-.003) .159	(-.007) .147	(-.004) .118	(-.006) .060	(-.002) .096	(-.003) .103	(-.008) -.054	(-.008) -.054	(-.008) -.011	(-.005) .025
(-.005) .138	(-.005) .086	(.000) .120	(-.004) .145	(-.004) .142	(.006) .128	(-.006) .118	(-.005) .057	(-.003) .095	(-.003) .104	(-.010) -.033	(-.010) -.033	(-.005) .004	(-.005) .038
(-.001) .134	(-.003) .087	(.000) .086	(-.002) .110	(-.002) .127	(-.003) .132	(-.003) .118	(-.002) .053	(.001) .090	(-.001) .105	(-.003) -.020	(-.003) -.020	(-.002) .016	(-.002) .047
(.003) .115	(.000) .082	(.001) .052	(.002) .069	(.004) .086	(.003) .103	(.001) .102	(.001) .040	(.004) .070	(.004) .086	(-.001) -.008	(-.001) -.008	(.001) .017	(.002) .041
(.000) .047	(.002) .050	(.000) .016	(.000) .022	(.003) .032	(.000) .041	(.000) .049	(-.011) .025	(.002) .025	(.002) .035	(-.001) -.003	(-.001) -.003	(.001) .005	(.001) .015
(-.004) .118	(-.004) .070	(-.001) .156	(-.006) .159	(-.005) .138	(-.008) .125	(-.006) .100	(-.005) .051	(-.003) .081	(-.004) .087	(-.007) -.052	(-.007) -.052	(-.006) -.015	(-.005) .019
(-.006) .123	(-.006) .077	(-.003) .120	(-.007) .145	(-.001) .133	(-.008) .129	(-.007) .108	(-.007) .057	(-.004) .088	(-.006) .097	(-.008) -.036	(-.008) -.036	(-.007) .002	(-.007) .035
(.000) .145	(-.003) .090	(.001) .092	(-.004) .125	(.003) .150	(-.002) .148	(-.003) .127	(-.003) .063	(.002) .101	(.000) .115	(-.002) -.024	(-.002) -.024	(-.002) .019	(.006) .060
.157	(-.002) .107	(.000) .065	(.001) .088	(.001) .116	(.000) .146	(-.002) .140	(-.004) .056	(.003) .097	(.003) .117	(-.002) -.009	(-.002) -.009	(.000) .026	(.001) .056
(.001) .107	.113	(.000) .038	(.002) .054	(.007) .079	(.003) .101	(.001) .122	(.001) .036	(.005) .067	(.005) .089	(-.001) -.003	(-.001) -.003	(.002) .019	(.004) .042
(-.001) .065	(.000) .038	.118	(-.001) .102	(.000) .080	(-.001) .069	(.000) .055	(.003) .025	(.000) .042	(.001) .047	(.000) -.048	(.000) -.048	(.004) -.020	(.001) .001
(.000) .088	(-.001) .054	(.002) .102	.130	(-.001) .114	(-.003) .100	(-.002) .081	(-.002) .050	(.001) .072	(.000) .078	(-.005) -.023	(-.005) -.023	(.000) .007	(.000) .033
(-.001) .116	(-.007) .079	(.000) .080	(.000) .114	.157	(-.002) .144	(-.003) .118	(-.005) .080	(.000) .114	(.001) .119	(-.005) -.008	(-.005) -.008	(-.002) .035	(.000) .066
(-.001) .146	(-.003) .101	(.001) .069	(.002) .100	(.002) .144	.194	(-.004) .171	(-.002) .076	(.005) .144	(.002) .164	(-.003) .003	(-.003) .003	(-.001) .052	(.002) .092
(.003) .140	(-.001) .122	(.000) .055	(.003) .081	(.002) .118	(.004) .171	.197	(-.002) .065	(.008) .124	(.010) .174	(-.001) .005	(-.001) .005	(.003) .048	(.004) .089
(.004) .056	(.000) .036	(-.002) .025	(.003) .050	(.004) .080	(.003) .076	(.001) .065	.091	(.008) .096	(.009) .085	(.000) .044	(.000) .044	(.005) .076	(.008) .086
(-.004) .097	(-.006) .067	(.000) .042	(.000) .072	(.000) .114	(-.005) .144	(-.008) .124	(-.008) .096	.190	(-.005) .183	(-.009) .047	(-.009) .047	(-.012) .119	(-.008) .163
(-.003) .117	(-.005) .089	(-.002) .047	(-.001) .078	(.000) .119	(-.002) .164	(-.010) .174	(-.009) .085	(.004) .183	.257	(-.006) .037	(-.006) .037	(-.006) .109	(-.006) .189
(.002) -.009	(.001) -.003	(-.001) -.048	(.004) -.023	(.005) -.008	(.004) .003	(.002) .005	(-.001) .044	(.010) .047	(.007) .037	.234	(.000) .234	(.001) .207	(.001) .142
(.002) -.009	(.001) -.003	(-.001) -.048	(.004) -.023	(.005) -.008	(.004) .003	(.002) .005	(-.001) .044	(.010) .047	(.007) .037	(.000) .234	.234	(.001) .207	(.001) .142
(-.001) .026	(-.003) .019	(-.004) -.020	(.001) .007	(.002) .035	(.001) .052	(-.003) .048	(-.005) .076	(.013) .119	(.005) .109	(-.002) .207	(-.002) .207	.284	(-.001) .260
(-.002) .056	(-.005) .042	(-.002) .001	(.000) .033	(.000) .066	(-.001) .092	(-.004) .089	(-.008) .086	(.008) .163	(.006) .189	(.000) .142	(.000) .142	(.001) .260	.396

TABLE 4.- INFLUENCE COEFFICIENTS FOR THE WING ON A THREE-POINT SUPPORT SYSTEM BASED ON A 1,000-POUND ANTISYMMETRICAL LOAD

[Stations are identified in figure 7]

Deflection station	Load station (a)																				
	7	8	9	10	11	12	13	14	15	16	17	18	19	20	21	23	24	25	26	27	28	29
7	0.053	(-0.004) .027	(-0.002) .017	(-0.001) .014	(0.001) .011	(0.007) .059	(0.003) .040	(0.002) .031	(0.007) .030	(0.001) .024	(0.004) .032	(0.001) .032	(0.006) .037	(0.007) .039	(0.007) .040	(0.001) .020	0.031	(0.003) .039	(-0.003) .001	(-0.003) .001	(0.000) .017	(0.004) .032
8	(.004) .027	.030	(.001) .022	(.002) .018	(.002) .015	(-.006) .034	(.003) .042	(.005) .036	(.006) .037	(.002) .032	(-.004) .022	(.000) .030	(.006) .040	(.007) .046	(.008) .050	(.004) .024	.036	(.003) .049	(.001) .004	(.001) .004	(.003) .023	(.007) .040
9	(.003) .017	(-.001) .022	.037	(.001) .029	(.001) .022	(-.004) .025	(-.003) .035	(.003) .050	(.005) .052	(.003) .047	(-.003) .017	(.000) .026	(.005) .046	(.004) .058	(.007) .064	(-.003) .022	.053	(-.002) .060	(.001) .005	(.001) .005	(.001) .026	(.003) .045
10	(.001) .014	(-.002) .018	(-.001) .029	.051	(.001) .038	(.000) .020	(.000) .030	(.002) .048	(.001) .072	(.002) .072	(-.001) .013	(.003) .023	(-.002) .047	(.002) .070	(.002) .088	(-.001) .030	.058	(-.001) .076	(.001) .010	(.001) .010	(-.001) .031	(-.001) .051
11	(-.002) .011	(-.002) .015	(-.001) .022	(-.001) .038	.056	(.001) .017	(.002) .025	(.000) .042	(.001) .063	(-.001) .090	(-.001) .011	(.003) .021	(.001) .043	(.001) .069	(-.004) .096	(.000) .030	.059	(-.003) .080	(.001) .012	(.001) .012	(.002) .033	(-.002) .053
12	(-.007) .059	(.005) .034	(.004) .025	(.000) .020	(-.002) .017	.109	(.000) .062	(.000) .046	(.003) .041	(.000) .036	(.001) .064	(-.003) .052	(.004) .054	(.005) .057	(.005) .056	(.000) .032	.048	(.001) .057	(-.003) -.001	(-.003) -.001	(.000) .024	(.004) .044
13	(-.002) .040	(-.002) .042	(.002) .035	(.000) .030	(-.001) .025	(.000) .062	.079	(.000) .067	(.003) .061	(.002) .056	(-.004) .043	(-.005) .060	(.003) .075	(.004) .081	(.005) .087	(.001) .048	.076	(-.003) .093	(.004) .012	(.004) .012	(-.001) .045	(.002) .072
14	(-.001) .031	(-.004) .036	(-.004) .050	(-.002) .048	(-.001) .042	(.000) .046	(.000) .067	.106	(.000) .101	(.000) .091	(-.005) .030	(.008) .053	(.000) .104	(-.001) .124	(.002) .132	(-.001) .063	.111	(-.003) .133	(.004) .024	(.004) .024	(-.007) .061	(-.005) .098
15	(-.006) .030	(-.006) .037	(-.005) .052	(-.002) .072	(-.002) .063	(-.003) .041	(-.003) .061	(.000) .101	.146	(.002) .136	(-.003) .026	(.007) .050	(.001) .103	(-.001) .158	(.005) .184	(-.001) .070	.132	(-.003) .169	(.003) .027	(.003) .027	(-.003) .074	(-.003) .115
16	(-.002) .024	(-.002) .032	(-.003) .047	(-.002) .072	(.001) .090	(-.001) .036	(-.002) .056	(.000) .091	(-.002) .136	.193	(-.003) .023	(.008) .047	(.001) .099	(.003) .163	(.000) .222	(-.001) .070	.140	(-.008) .190	(.003) .032	(.003) .032	(.006) .081	(-.007) .126
17	(-.004) .032	(.004) .022	(.003) .017	(.002) .013	(.000) .011	(-.001) .064	(.004) .043	(.005) .030	(.003) .026	(.003) .023	.071	(-.017) .039	(-.003) .038	(-.002) .036	(-.004) .035	(-.003) .018	.035	(-.006) .035	(-.003) -.019	(-.003) -.019	(-.006) .004	(-.005) .016
18	(-.001) .032	(-.001) .030	(.000) .026	(-.002) .023	(-.002) .021	(.004) .052	(.006) .060	(-.008) .053	(-.007) .050	(-.008) .047	(.017) .039	.070	(.020) .081	(.011) .070	(.022) .082	(.006) .044	.057	(.012) .080	(-.002) .008	(-.002) .008	(.005) .037	(.011) .061
19	(-.006) .037	(-.007) .040	(-.005) .046	(.001) .047	(-.001) .043	(-.004) .054	(-.002) .075	(.000) .104	(-.001) .103	(-.001) .099	(.004) .038	(-.020) .081	.149	(.001) .154	(.007) .150	(.000) .093	.151	(-.005) .170	(.004) .033	(.004) .033	(-.007) .087	(-.005) .130
20	(-.007) .039	(-.007) .046	(-.004) .058	(-.001) .070	(-.002) .069	(-.006) .057	(-.003) .081	(.001) .124	(.002) .158	(-.004) .163	(.003) .036	(-.012) .070	(-.001) .154	.254	(.001) .261	(.001) .109	.228	(-.008) .267	(.008) .051	(.008) .051	(-.009) .122	(-.010) .188
21	(-.007) .040	(-.008) .050	(-.006) .064	(-.003) .088	(.004) .096	(-.005) .056	(-.006) .087	(-.002) .132	(-.006) .184	(.001) .222	(.003) .035	(-.022) .082	(-.007) .150	(-.002) .261	.343	(-.001) .112	.237	(-.013) .321	(.005) .053	(.005) .053	(.003) .141	(.009) .231
23	(-.001) .020	(-.004) .024	(.002) .022	(.001) .030	(.000) .030	(-.001) .032	(-.001) .048	(.002) .063	(.002) .070	(.001) .070	(.004) .018	(-.007) .044	(-.001) .093	(-.001) .109	(.001) .112	.107	.148	(-.009) .140	(.002) .061	(.002) .061	(-.007) .109	(-.005) .138
24	.031	.036	.053	.058	.059	.048	.076	.111	.132	.140	.035	.057	.151	.228	.237	.148	-----(b)	.308	.082	.082	.190	.269
25	(-.003) .039	(-.004) .049	(.001) .060	(.002) .076	(.003) .080	(.000) .057	(.002) .093	(.004) .133	(.002) .169	(.008) .190	(.006) .035	(-.011) .080	(.004) .170	(.008) .267	(.014) .321	(.010) .140	.308	.428	(.001) .088	(.001) .088	(.028) .221	(.024) .289
26	(.003) .001	(.000) .004	(-.001) .005	(-.001) .010	(-.001) .012	(.002) -.001	(-.003) .012	(-.005) .024	(-.003) .027	(-.003) .032	(.002) -.019	(.001) .008	(-.004) .033	(-.008) .051	(-.005) .053	(-.001) .061	.082	(-.002) .088	.203	(.000) .203	(-.002) .195	(.015) .173
27	(.003) .001	(.000) .004	(-.001) .005	(-.001) .010	(-.001) .012	(.002) -.001	(-.003) .012	(-.005) .024	(-.003) .027	(-.003) .032	(.002) -.019	(.001) .008	(-.004) .033	(-.008) .051	(-.005) .053	(-.001) .061	.082	(-.002) .088	(.000) .203	.203	(-.002) .195	(.015) .173
28	(.000) .017	(-.003) .023	(-.001) .026	(.002) .031	(-.001) .033	(.000) .024	(.002) .045	(.008) .061	(.003) .074	(-.007) .081	(.006) .004	(-.004) .037	(.006) .087	(.009) .122	(-.003) .141	(.007) .109	.190	(-.027) .221	(.002) .195	(.002) .195	.302	(.022) .331
29	(-.005) .032	(-.007) .040	(-.004) .045	(.002) .051	(.002) .053	(-.004) .044	(-.002) .072	(.004) .098	(.003) .115	(.008) .126	(.005) .016	(-.011) .061	(.005) .130	(.009) .188	(-.009) .231	(.005) .138	.269	(-.024) .289	(-.015) .173	(-.015) .173	(-.022) .331	.528

[a]Values in parentheses are deviations from the mean value.
[b]Deflection of station 24 due to a load at station 24 was not measured.

TABLE 5.- WEIGHT DISTRIBUTION OF DELTA WING

Station (see fig. 7)	Weight, lb					
	Ribs	Skins	Concentrated	Spars	Rivets	Total
1	0.2208	1.0224	0.0563	0.0980	0.0157	1.3996
2	.5687	1.8764	.1068	.1400	.0254	2.7622
3	.6586	2.1538	------	.1345	.0202	2.9672
4	.7146	2.3812	------	.0990	.0221	3.2127
5	.6071	2.2202	.4556	.1243	.0263	3.4801
6	.2059	1.6776	.1182	------	.0099	1.9379
7	.2748	.7366	------	.2156	.0136	1.2572
8	1.0019	1.3006	------	.2708	.0409	2.6096
9	.7935	1.6660	------	.2236	.0272	2.6808
10	.5042	1.8506	------	.1953	.0207	1.1148
11	.5171	2.7766	------	.2982	.0282	5.0935
12	.0759	.6084	------	.2548	.0094	.9376
13	.2696	1.1468	------	.3735	.0197	1.8677
14	.3480	1.5232	------	.3002	.0160	2.1639
15	.3311	1.7584	------	.2695	.0174	.5962
16	.3247	3.5818	------	.4308	.0258	6.1196
17	.0324	.3730	1.2680	.2744	.0094	1.6453
18	.1314	.8046	------	.4669	.0160	1.7775
19	.1905	1.2222	------	.3668	.0122	1.7669
20	.1741	1.4392	------	.3389	.0136	.5718
21	.1589	2.7778	------	.5591	.0225	4.8903
22	.0571	.4966	1.4619	.5116	.0127	2.0576
23	.0939	.7070	------	.4119	.0089	1.7214
24	.0897	.8698	------	.3914	.0099	.4462
25	.0870	1.7678	------	.6577	.0174	3.4271
26	.0035	.0422	------	.1202	.0047	.1855
27	.0356	.2076	------	.2138	.0033	.4600
28	.0570	.2660	------	.2499	.0038	.2555
29	.0136	.5764	------	.5068	.0075	1.4108
Total	8.5412	39.8308	3.4668	8.4965	0.4804	60.8161

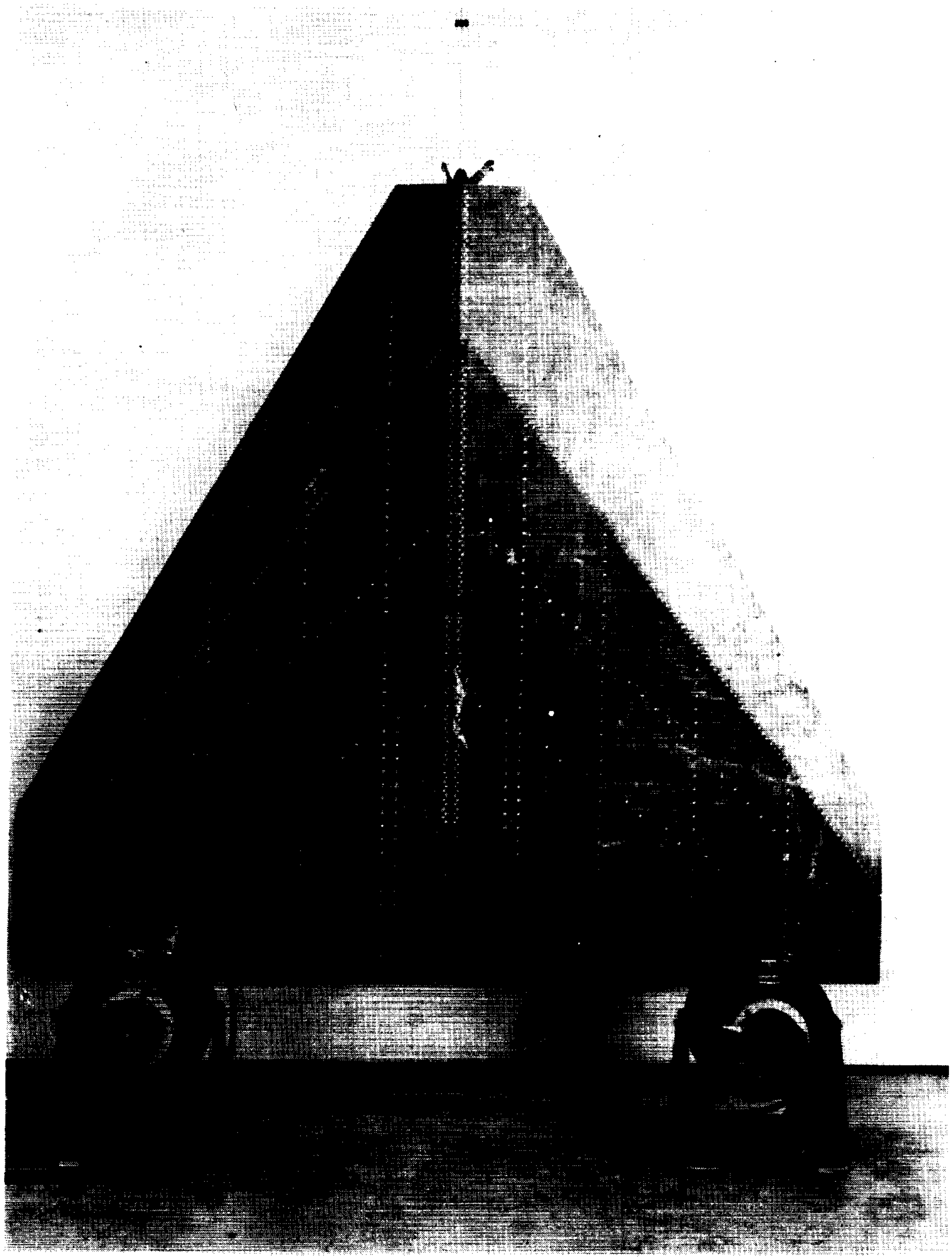

Figure 1.- Delta-wing test specimen. L-58-1458

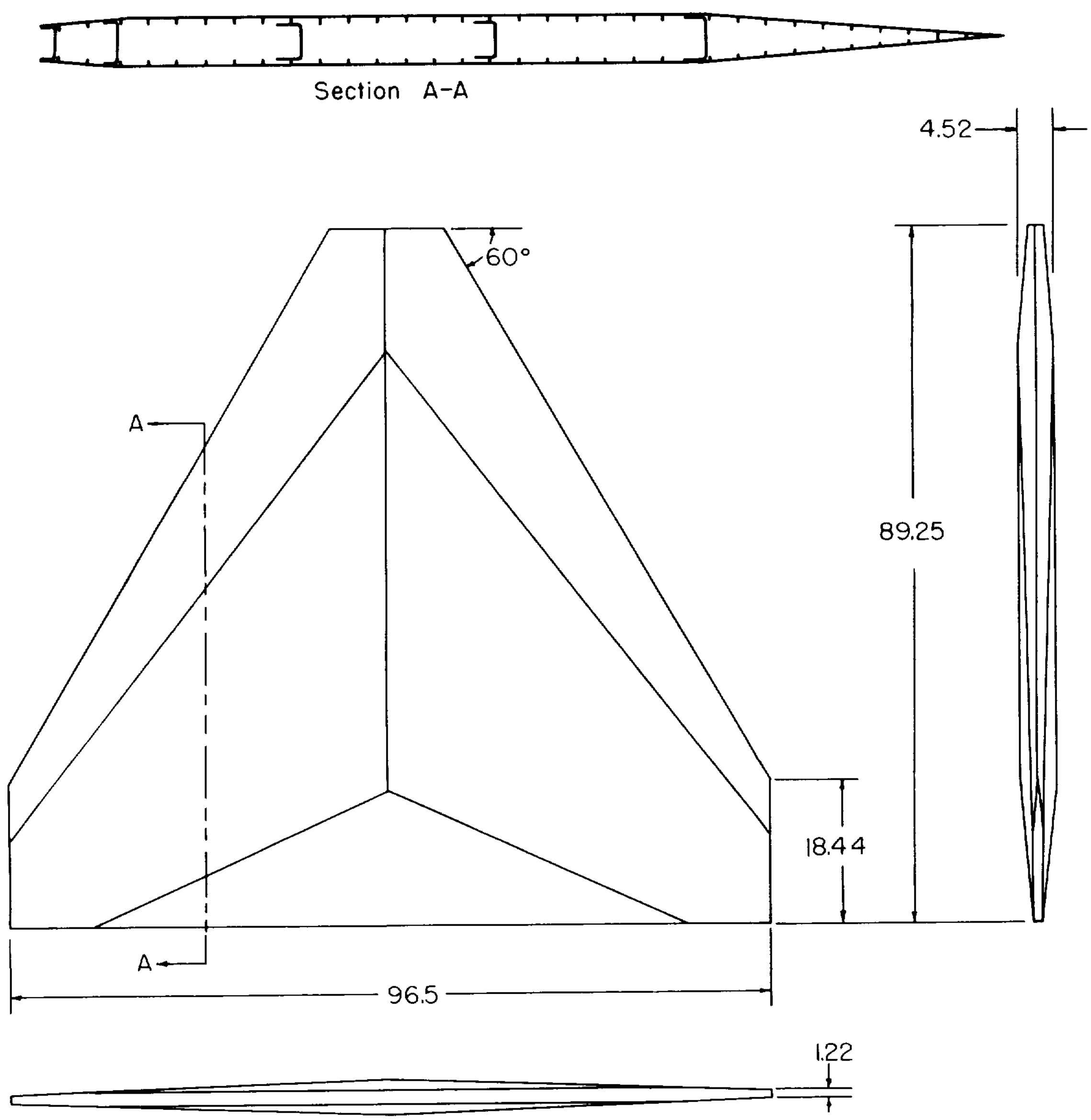

(a) Overall view.

Figure 2.- Nominal dimensions of the delta-wing specimen. All dimensions are in inches.

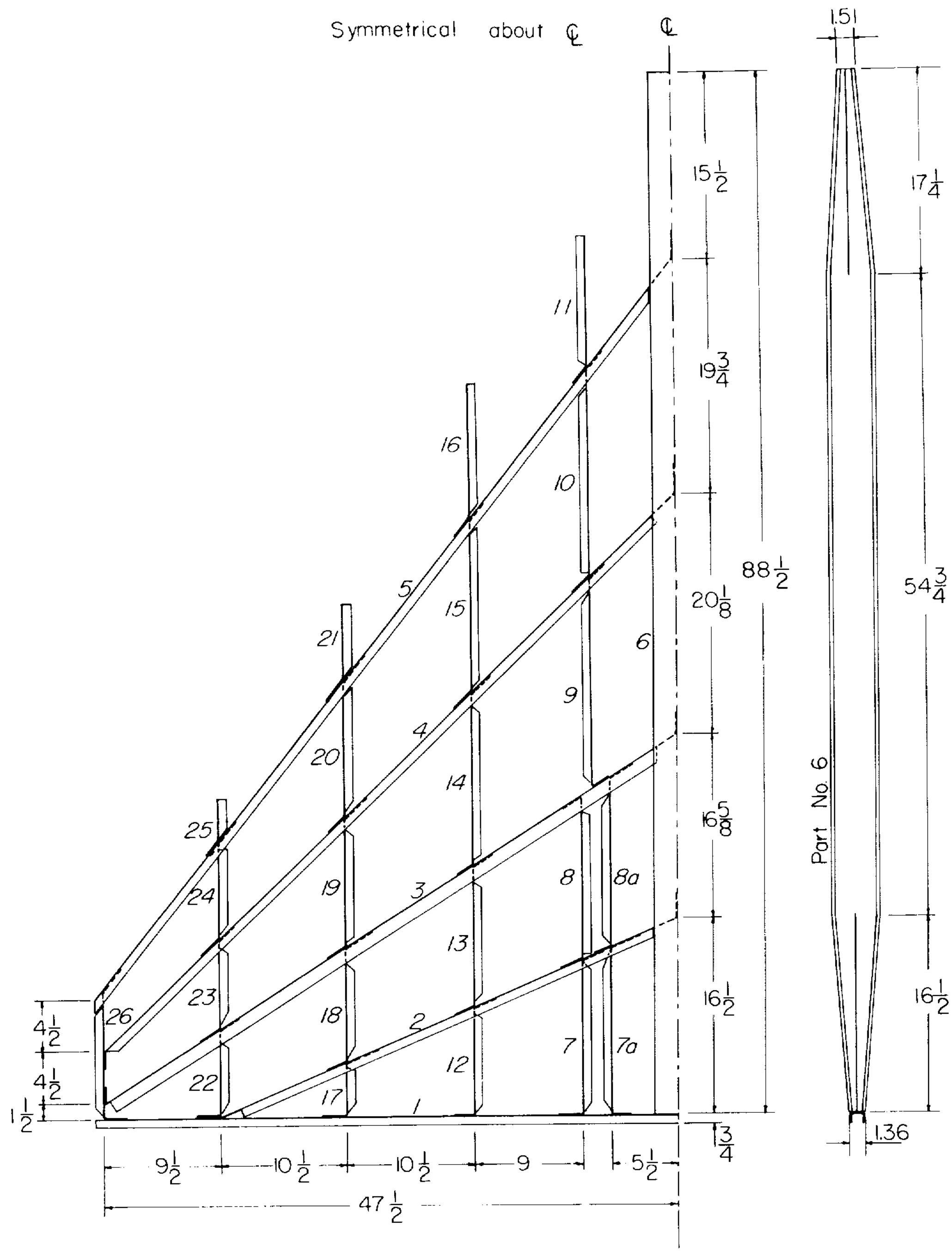

(b) Internal construction.

Figure 2.- Continued.

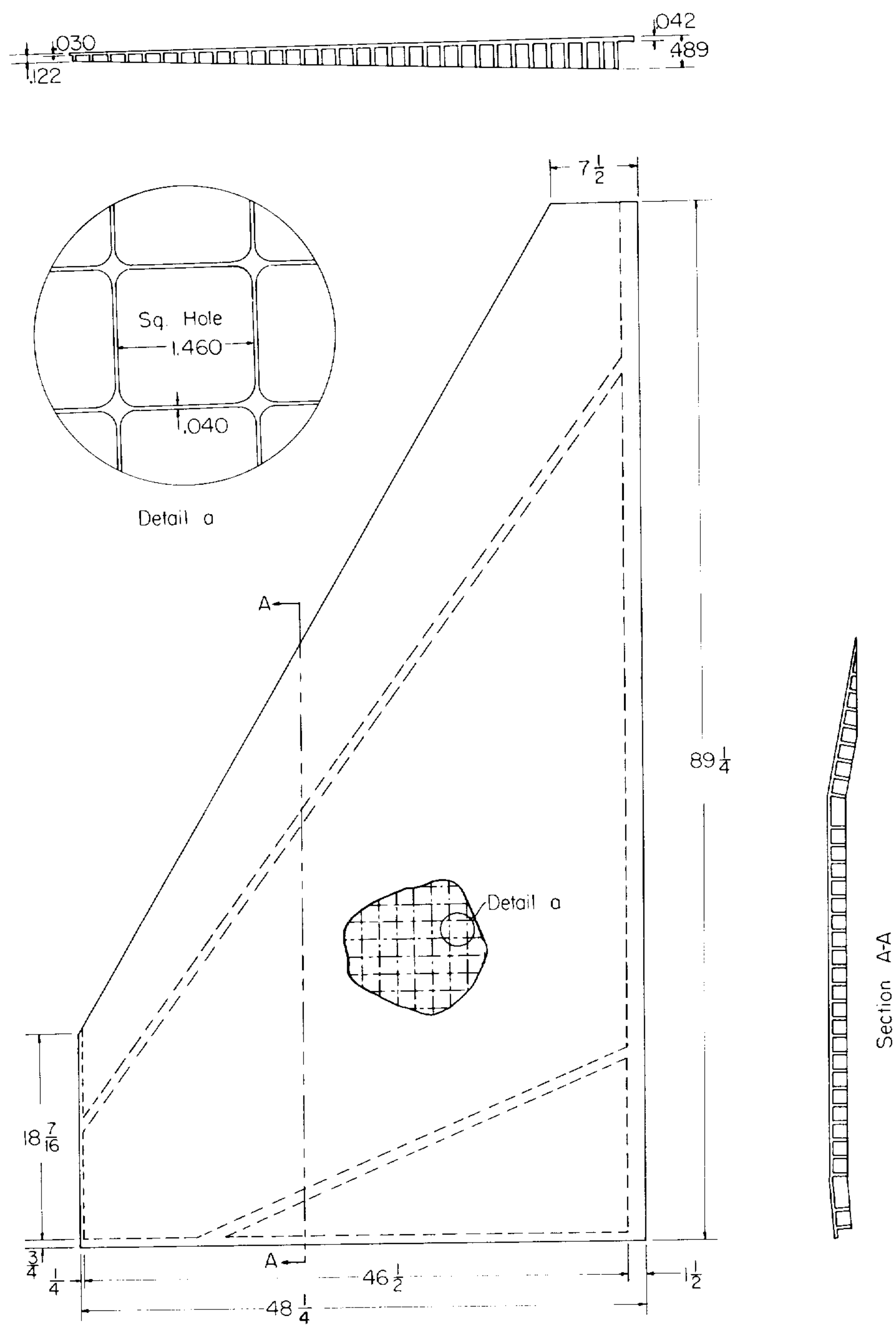

(c) Average dimensions of covers.

Figure 2.- Concluded.

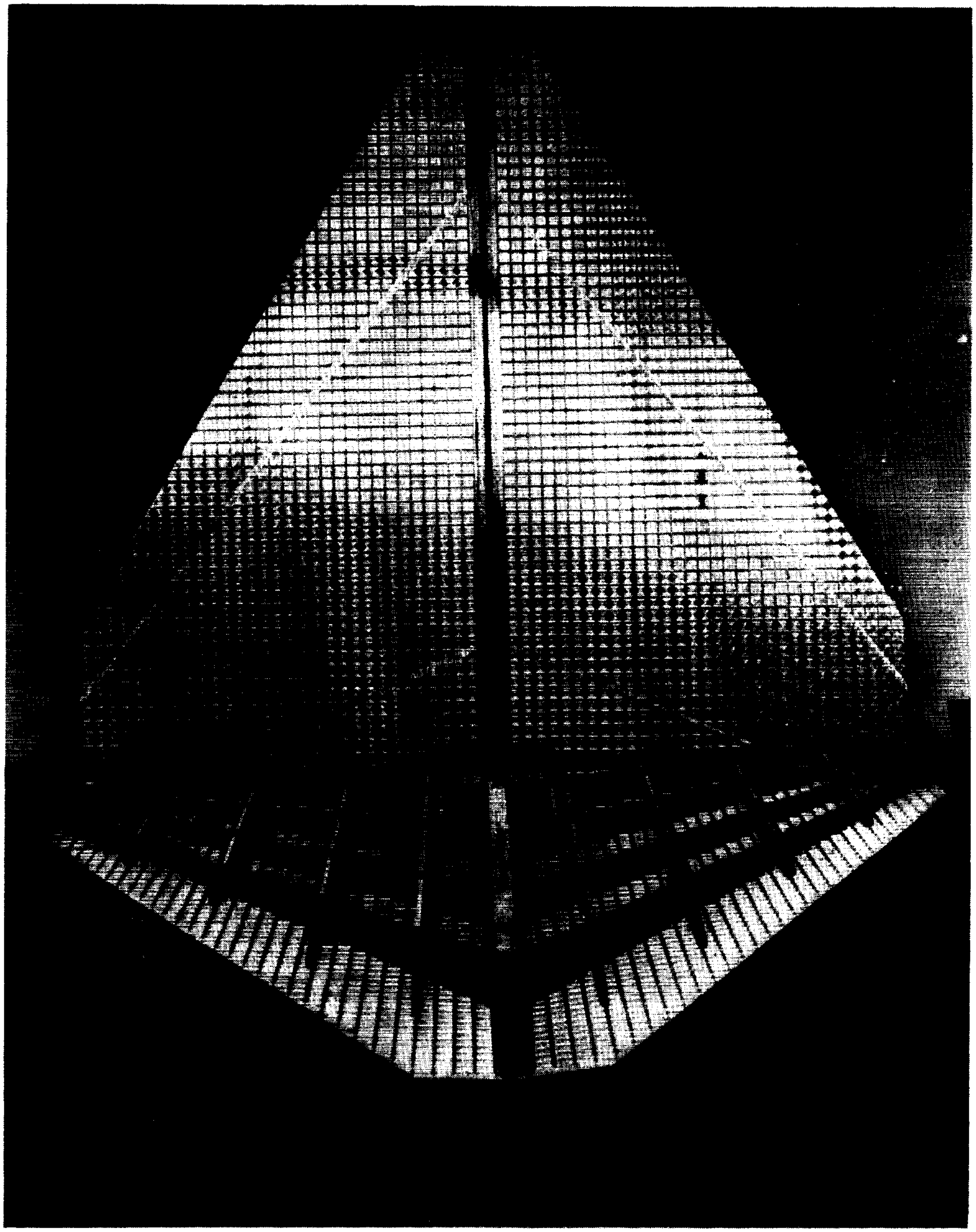

Figure 3.- Wing-specimen assembly. L-89951

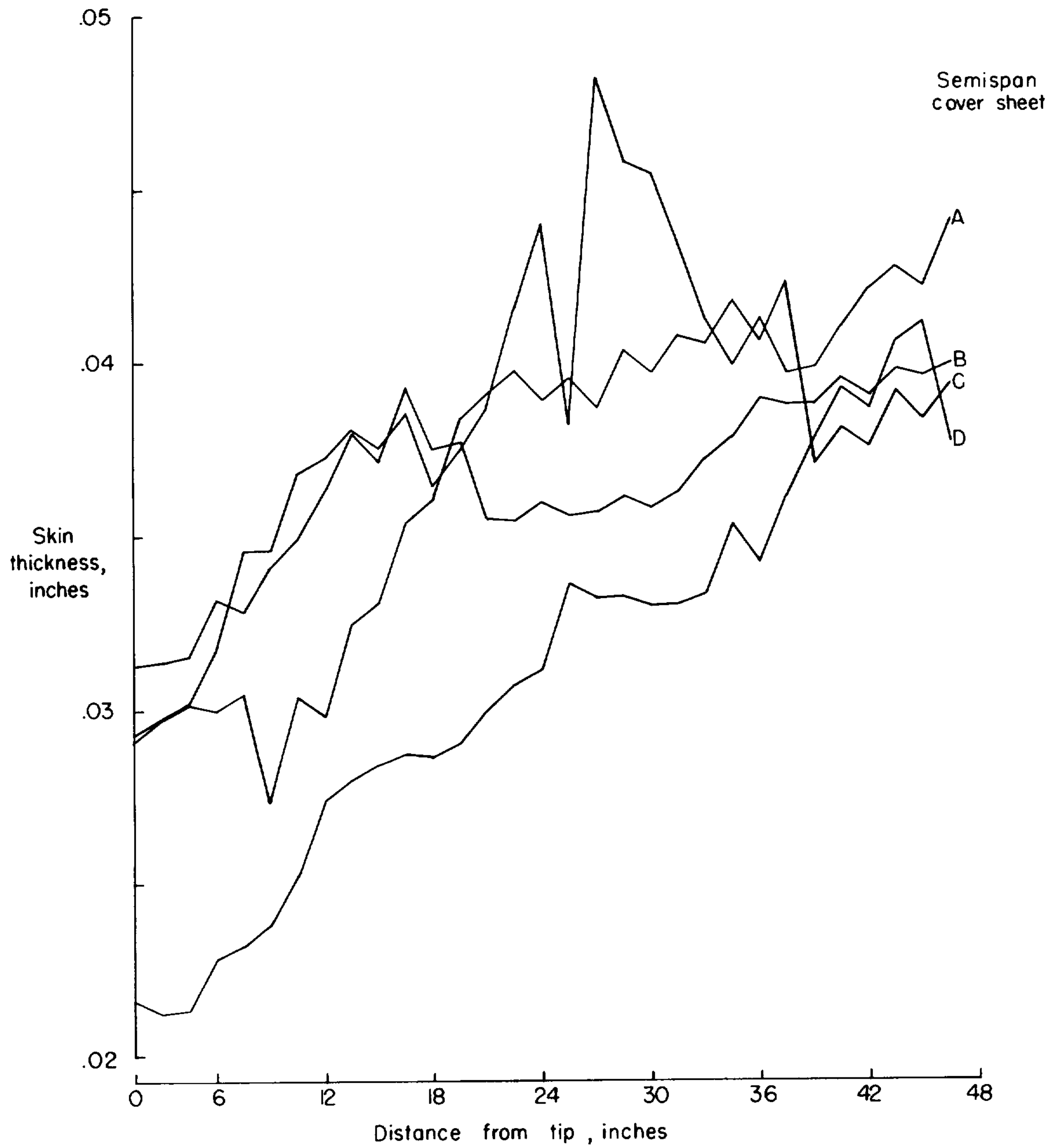

Figure 4.- Spanwise variation of average chordwise skin thicknesses.

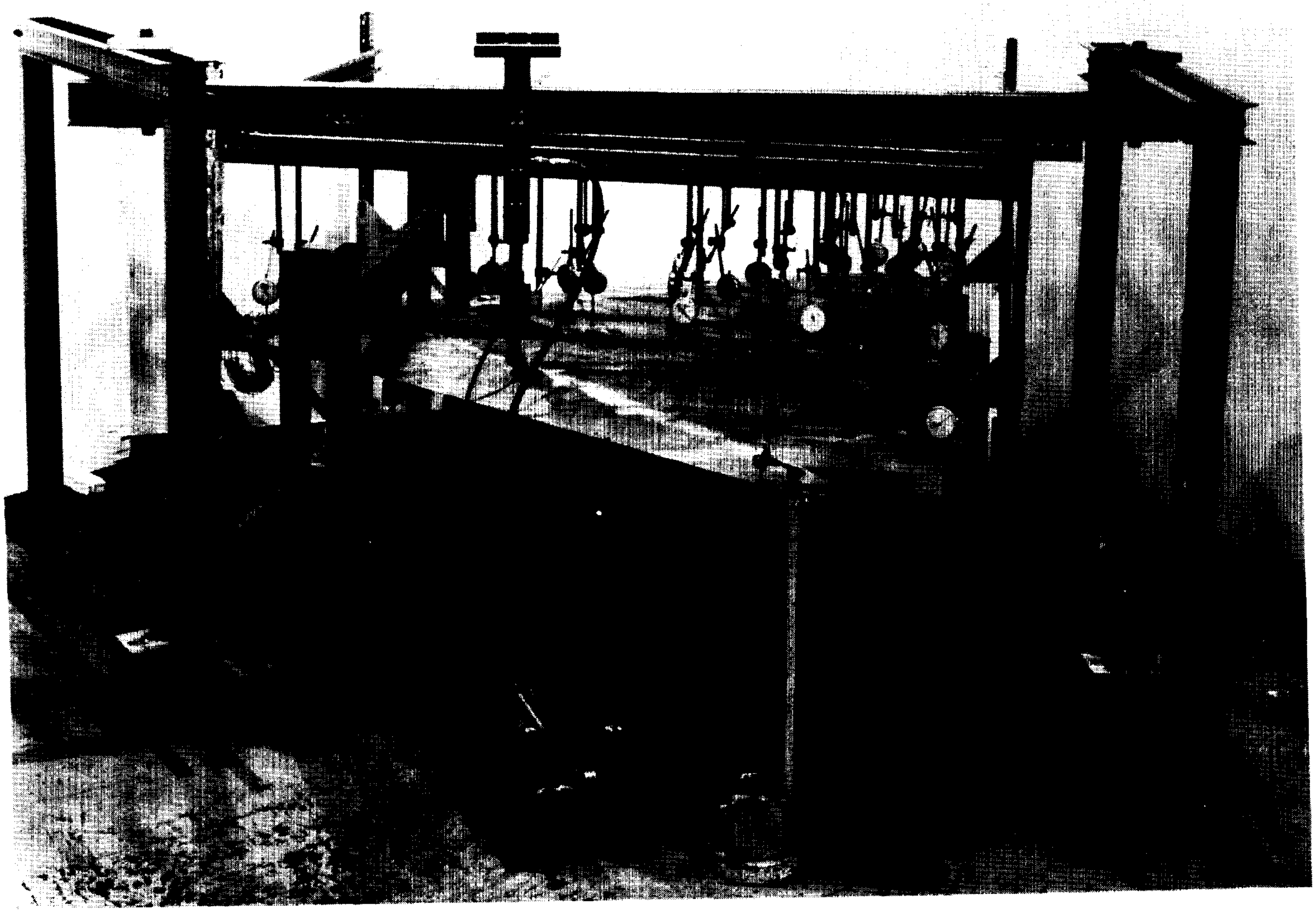

Figure 5.- Static-test setup. L-94049

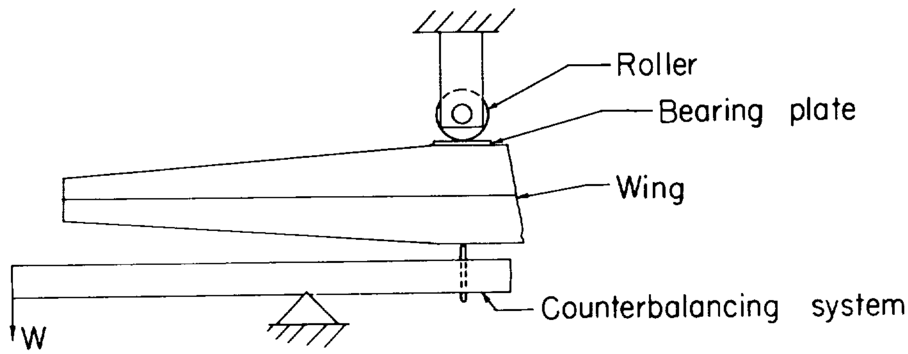

(a) Forward support.

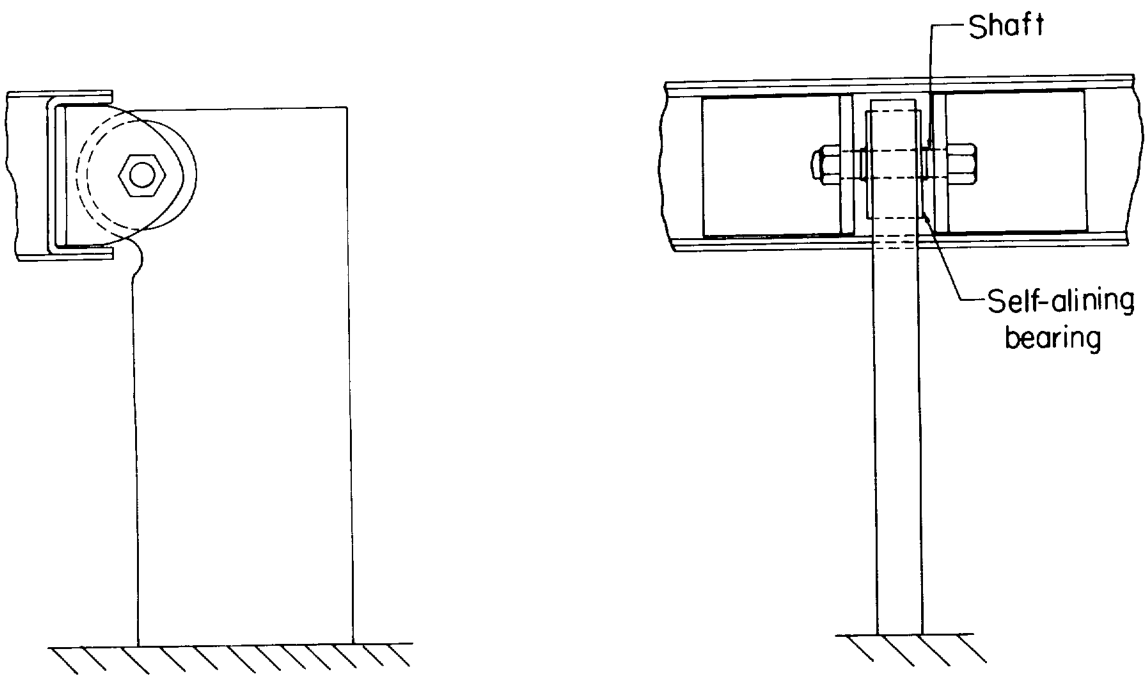

(b) Rear supports.

Figure 6.- Support fixtures.

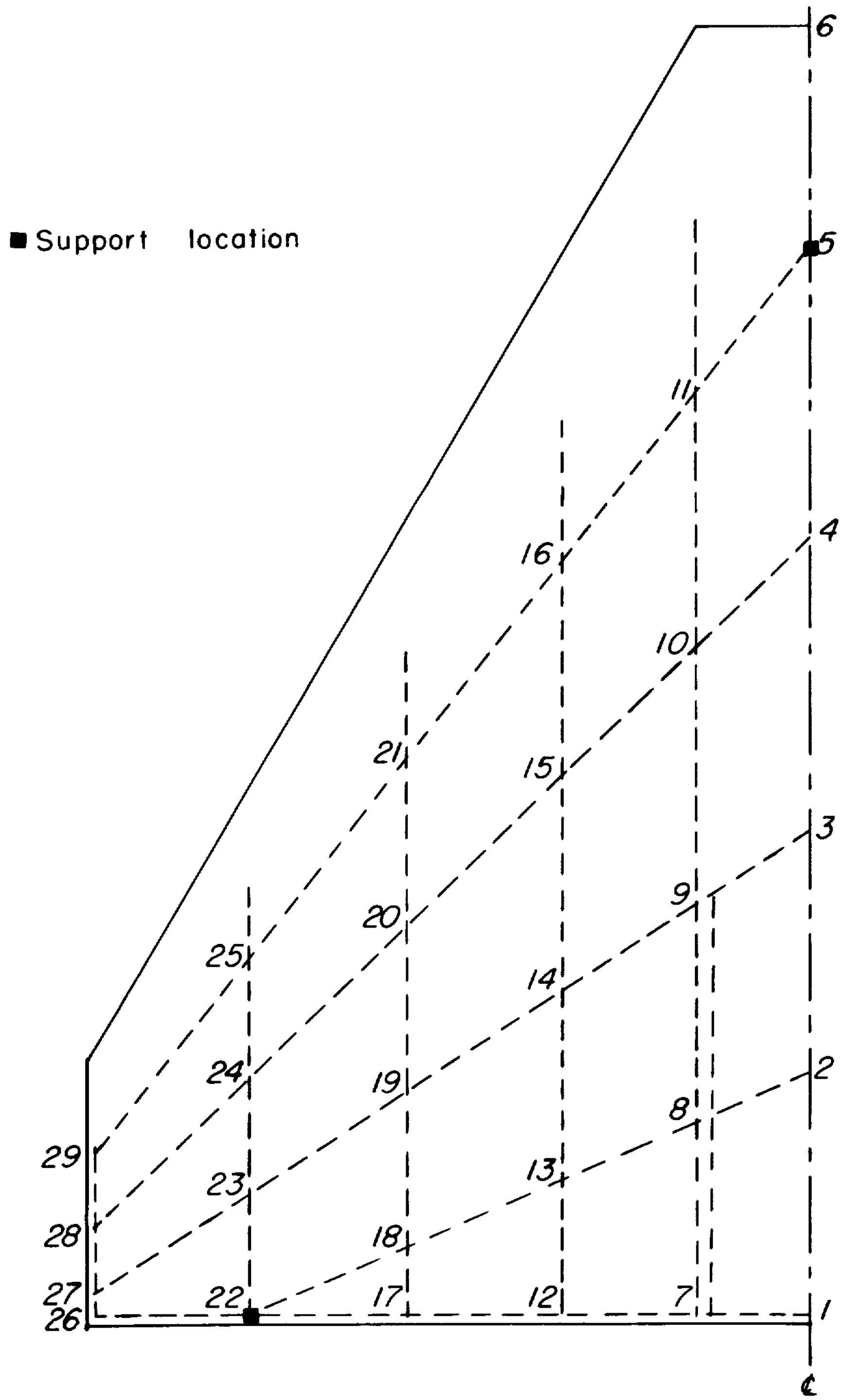

Figure 7.- Station locations.

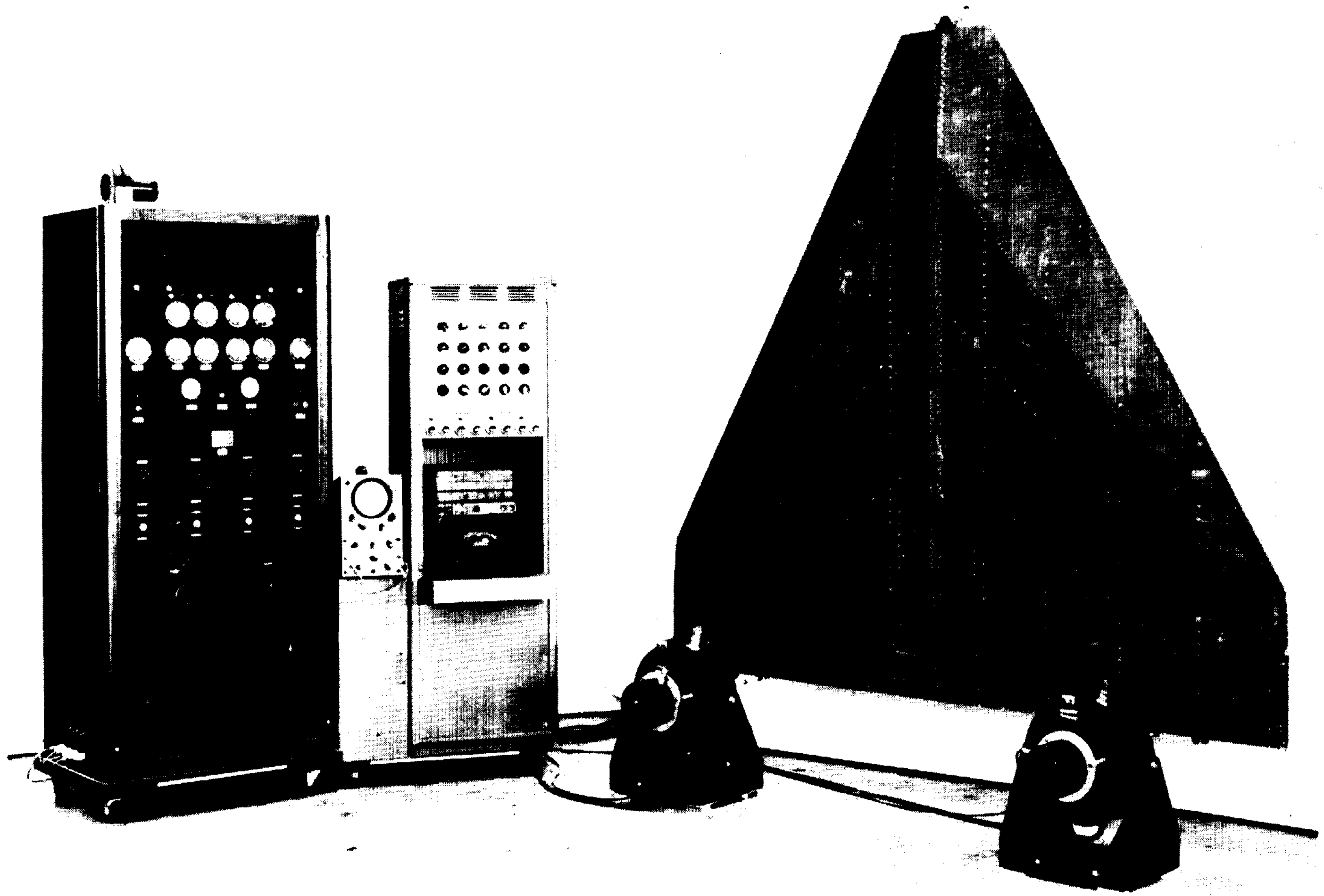

Figure 8.- Vibration test setup. L-58-1457

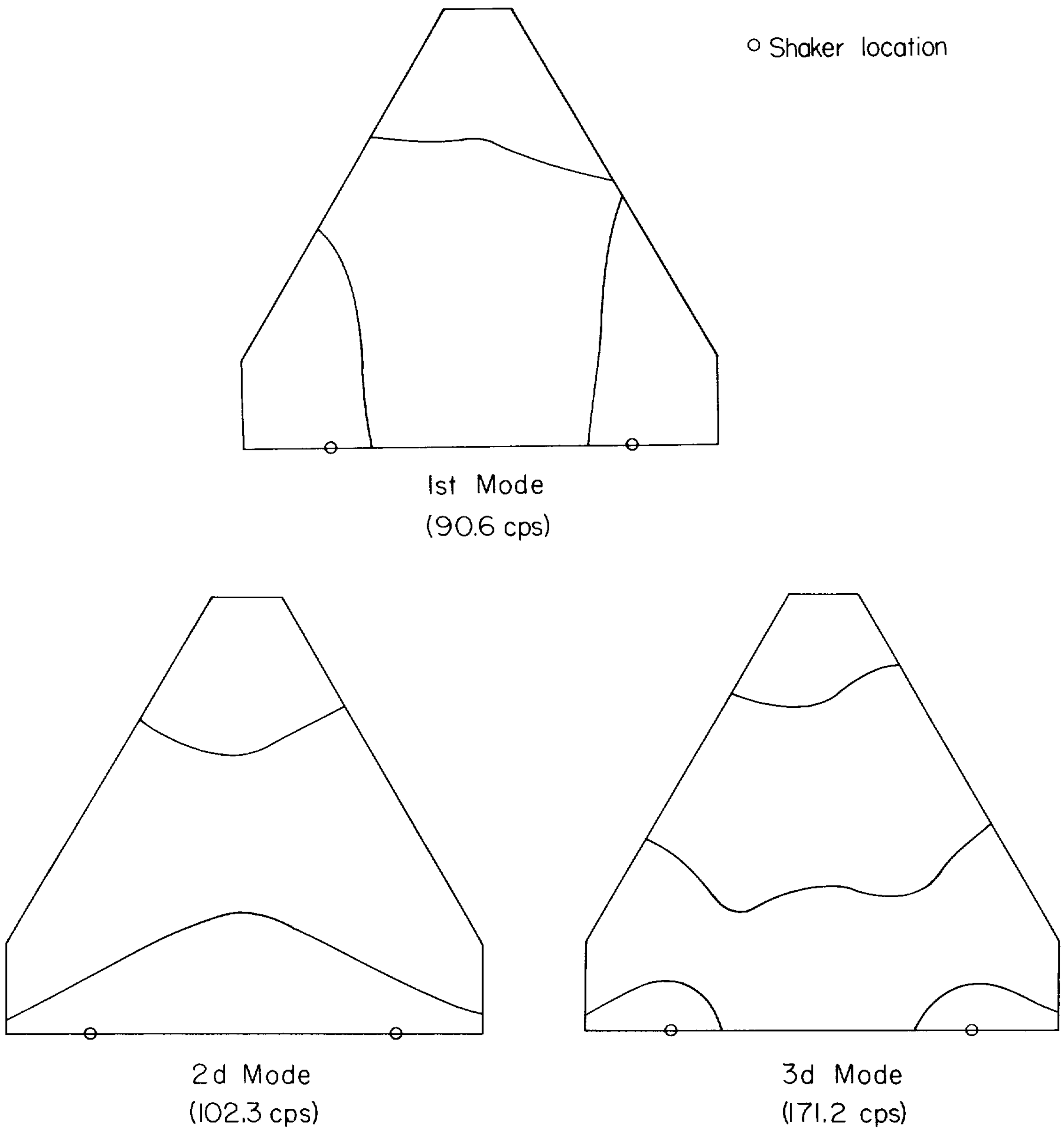

(a) Symmetrical.

Figure 9.- Modes and frequencies of delta-wing specimen (experimental).

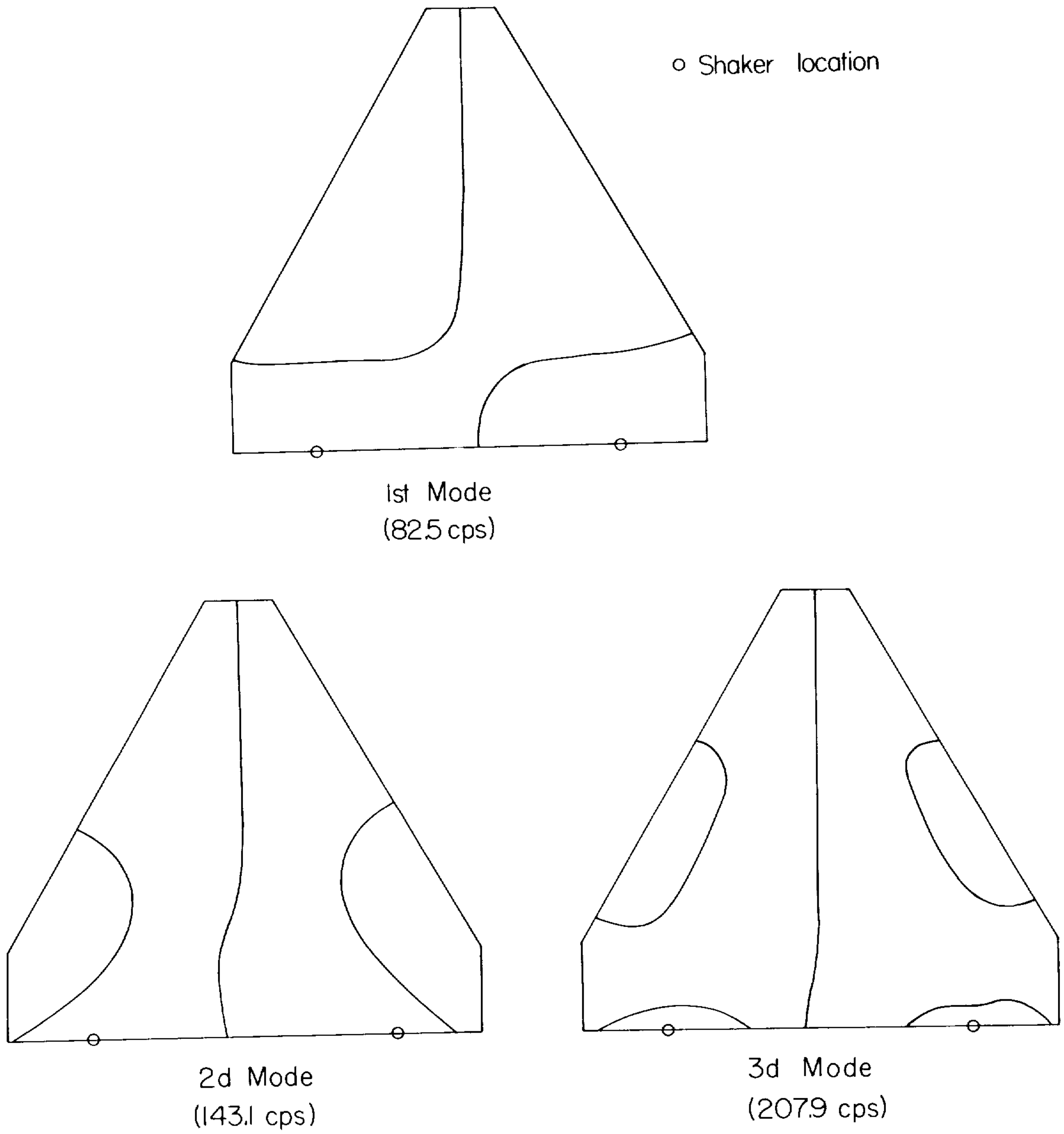

(b) Antisymmetrical.

Figure 9.- Concluded.

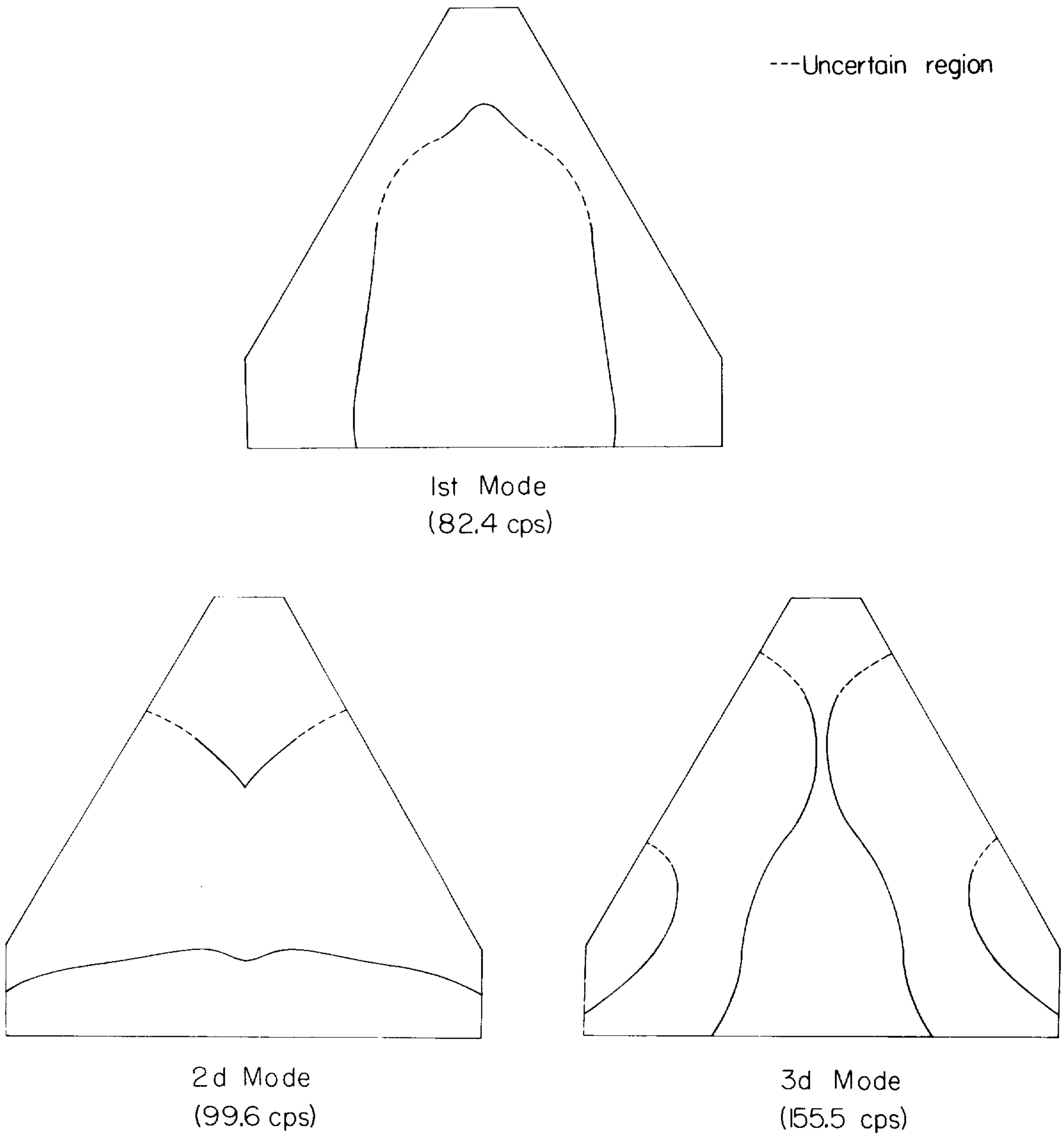

Figure 10.- Modes and frequencies of delta-wing specimen (calculated from the symmetrical influence coefficients).

NASA MEMO 2-4-59L
National Aeronautics and Space Administration.
EXPERIMENTAL INFLUENCE COEFFICIENTS AND VIBRATION MODES OF A MULTISPAR 60° DELTA WING. Deene J. Weidman and Eldon E. Kordes. May 1959. 28p. diagrs., photos., tabs. (NASA MEMORANDUM 2-4-59L)

Test results are presented for both symmetrical and antisymmetrical static loading of a wing model mounted on a three-point support system. The first six free-free vibration modes were determined experimentally. A comparison is made of the symmetrical nodal patterns and frequencies with the symmetrical nodal patterns and frequencies calculated from the experimental influence coefficients.

Copies obtainable from NASA, Washington

1. Vibration and Flutter (4.2)
2. Loads and Stresses, Structural (4.3.7)
I. Weidman, Deene J.
II. Kordes, Eldon E.
III. NASA MEMO 2-4-59L

NASA

NASA MEMO 2-4-59L
National Aeronautics and Space Administration.
EXPERIMENTAL INFLUENCE COEFFICIENTS AND VIBRATION MODES OF A MULTISPAR 60° DELTA WING. Deene J. Weidman and Eldon E. Kordes. May 1959. 28p. diagrs., photos., tabs. (NASA MEMORANDUM 2-4-59L)

Test results are presented for both symmetrical and antisymmetrical static loading of a wing model mounted on a three-point support system. The first six free-free vibration modes were determined experimentally. A comparison is made of the symmetrical nodal patterns and frequencies with the symmetrical nodal patterns and frequencies calculated from the experimental influence coefficients.

Copies obtainable from NASA, Washington

1. Vibration and Flutter (4.2)
2. Loads and Stresses, Structural (4.3.7)
I. Weidman, Deene J.
II. Kordes, Eldon E.
III. NASA MEMO 2-4-59L

NASA

NASA MEMO 2-4-59L
National Aeronautics and Space Administration.
EXPERIMENTAL INFLUENCE COEFFICIENTS AND VIBRATION MODES OF A MULTISPAR 60° DELTA WING. Deene J. Weidman and Eldon E. Kordes. May 1959. 28p. diagrs., photos., tabs. (NASA MEMORANDUM 2-4-59L)

Test results are presented for both symmetrical and antisymmetrical static loading of a wing model mounted on a three-point support system. The first six free-free vibration modes were determined experimentally. A comparison is made of the symmetrical nodal patterns and frequencies with the symmetrical nodal patterns and frequencies calculated from the experimental influence coefficients.

Copies obtainable from NASA, Washington

1. Vibration and Flutter (4.2)
2. Loads and Stresses, Structural (4.3.7)
I. Weidman, Deene J.
II. Kordes, Eldon E.
III. NASA MEMO 2-4-59L

NASA

NASA MEMO 2-4-59L
National Aeronautics and Space Administration.
EXPERIMENTAL INFLUENCE COEFFICIENTS AND VIBRATION MODES OF A MULTISPAR 60° DELTA WING. Deene J. Weidman and Eldon E. Kordes. May 1959. 28p. diagrs., photos., tabs. (NASA MEMORANDUM 2-4-59L)

Test results are presented for both symmetrical and antisymmetrical static loading of a wing model mounted on a three-point support system. The first six free-free vibration modes were determined experimentally. A comparison is made of the symmetrical nodal patterns and frequencies with the symmetrical nodal patterns and frequencies calculated from the experimental influence coefficients.

Copies obtainable from NASA, Washington

1. Vibration and Flutter (4.2)
2. Loads and Stresses, Structural (4.3.7)
I. Weidman, Deene J.
II. Kordes, Eldon E.
III. NASA MEMO 2-4-59L

NASA